actuators

MDPI

Article

Machine-Knitted Seamless Pneumatic Actuators for Soft Robotics: Design, Fabrication, and Characterization

Hend M. Elmoughni [1,†], Ayse Feyza Yilmaz [1,†], Kadir Ozlem [2,†], Fidan Khalilbayli [2,†], Leonardo Cappello [3,4], Asli Tuncay Atalay [5], Gökhan Ince [2] and Ozgur Atalay [1,*]

1 Faculty of Textile Technologies and Design, Istanbul Technical University, Istanbul 34437, Turkey; hend.elmoughni@gmail.com (H.M.E.); yilmazaysef@itu.edu.tr (A.F.Y.)
2 Computer Engineering Department, Istanbul Technical University, Istanbul 34469, Turkey; kadir.ozlem@itu.edu.tr (K.O.); khalilbayli15@itu.edu.tr (F.K.); gokhan.ince@itu.edu.tr (G.I.)
3 The BioRobotics Institute, Scuola Superiore Sant'Anna, 56127 Pisa, Italy; leonardo.cappello@santannapisa.it
4 Department of Excellence in Robotics & AI, Scuola Superiore Sant'Anna, The BioRobotics Institute, 56127 Pisa, Italy
5 Faculty of Technology, Textile Engineering Department, Marmara University, Istanbul 34722, Turkey; asli.atalay@marmara.edu.tr
* Correspondence: atalayoz@itu.edu.tr
† These authors contributed equally to this work.

Abstract: Computerized machine knitting offers an attractive fabrication technology for incorporating wearable assistive devices into garments. In this work, we utilized, for the first time, whole-garment knitting techniques to manufacture a seamless fully knitted pneumatic bending actuator, which represents an advancement to existing cut-and-sew manufacturing techniques. Various machine knitting parameters were investigated to create anisotropic actuator structures, which exhibited a range of bending and extension motions when pressurized with air. The functionality of the actuator was demonstrated through integration into an assistive glove for hand grip action. The achieved curvature range when pressurizing the actuators up to 150 kPa was sufficient to grasp objects down to 3 cm in diameter and up to 125 g in weight. This manufacturing technique is rapid and scalable, paving the way for mass-production of customizable soft robotics wearables.

Keywords: soft robotics; knitted actuators; wearables; assistive devices

Citation: Elmoughni, H. M.; Yilmaz, A. F.; Ozlem, K.; Khalilbayli, F.; Cappello, L.; Tuncay Atalay, A.; Ince, G.; Atalay, O. Machine-Knitted Seamless Pneumatic Actuators for Soft Robotics: Design, Fabrication,and Characterization. *Actuators* **2021**, *10*, 94. https://doi.org/10.3390/act10050094

Academic Editor: Alessio Merola

Received: 9 March 2021
Accepted: 9 April 2021
Published: 30 April 2021

1. Introduction

Soft wearable robotic technologies have seen tremendous research efforts in the past decade as an attractive solution for human mobility assistance and rehabilitation [1–3]. The use of soft materials that conform to the human body and are compliant when exposed to external forces has led to the gradual advancement from rigid exoskeletons to lighter weight soft wearable alternatives [4–8]. Namely, garment-like textile-based fluidic actuators demonstrated promising potential towards increased user comfort and safety [9–11]. Unlike elastomeric and tendon actuators, which are heavier and bulkier, textile-based actuators can be easily concealed thanks to their reduced weight and volume. Various methodologies have been presented to date to create pneumatic bending textile-based actuators, which translated successfully into low-cost wearable assistive devices [12–17]. The efforts in this context have mainly focused on creating anisotropic structures through combining a highly extensible top material with an inextensible base layer to form the inflatable bending textile pouches. The contrasting mechanical properties of the combined layers cause the actuator to exhibit bending motions upon pressurizing with compressed fluid such as air [13,18]. The techniques used to connect the layers follow a cut-and-sew approach and rely heavily on manual assembly and fabrication steps. The process is not only time consuming and labor intensive, but it also presents other challenges including

inconsistencies and the possible failure of the actuator during inflation. Another major drawback of the process is that the actuator behavior is determined by off-the-shelf textile material's properties, which are usually controlled at the mass-production scale, limiting systematic iterations and fine-tuning. Computerized machine knitting offers an alternative end-to-end automated fabrication technology that can be leveraged to produce soft textile actuators with the desired deformations. Despite the advanced capabilities of industrial machine knitting to produce fully shaped garments with minimal post-processing, this technology is seldom explored as a fabrication technology for wearable assistive soft robotics devices. In this work, we manufactured a proof-of-concept fully knitted seamless bending actuator using machine knitting. The knitting parameters were varied to produce four tubular 3D structures with different stretch properties at the top and bottom layers to create anisotropy. Experimental results showed that the actuators exhibited a range of bending behaviors comparable to previously reported cut-and-sew textile actuators. Finally, to demonstrate the potential of the developed seamless knitted actuator, five actuators were used to construct an assistive glove, which was capable of gripping and holding various objects at pressure range up to 150 kPa. We recorded surface electromyography (EMG) signals to detect muscle activity on a healthy subject wearing the glove, which showed that the knitted actuators exerted an auxiliary bending force capable of assisting the hand motion and grasping activities of daily living.

2. Machine-Knitted Actuator Fabrication and Design

Knitting is a textile fabrication process based on forming a yarn into rows (courses) and columns (wales) of loops or stitches [19]. In its most basic form, a knitted structure can be formed from a single continuous length of yarn. Flat-bed machine knitting is the most widely used mechanical process for knitted fabric manufacturing and is considered by far the most accessible for rapid textile prototyping. The machine forms a knitted structure through a sliding action of multiple needles arranged in parallel on a flat bed. The machine gauge defines the number of needles per inch on the needle bed; therefore, it determines the fabric thickness that can be produced. Finer fabrics can be knitted on high-gauge machines (12–18 needles per inch), while coarser fabrics can be knitted on lower gauge machines. In machine knitting, the needles' action is synchronized with yarn carriers that provide yarn to the needle hook, which grabs the yarn to form the stitch and pulls it through the previously held loop (Figure 1a) [20]. This structure of inter-looped yarn gives knitted fabrics their inherent stretch property. Digitally controlled machines enable controlling the needle action and the movement of multiple yarn carriers simultaneously. This allows knitting of different yarns independently at digitally pre-set knitting parameters to produce single or multiple layers with different properties. The type of yarn used, stitch density, and needle action selected are all knitting machine parameters that determine the mechanical properties of the produced fabric. Advanced computerized knitting machines are also capable of whole-garment knitting, which allows for manufacturing seamless garments without the need for the labor-intensive cutting and sewing processes [21]. In this work, we leveraged computerized knitting, employing a 10-gauge SHIMA SEIKI whole-garment knitting machine to manufacture seamless knitted actuators. The basic actuator structure consisted of a knitted pouch construction with two chambers. For the purposes of this work, bending was the desired deformation; therefore, an anisotropic actuator fabric structure was designed. The stitch density and the type of yarn constituted the two knitting parameters that were varied to control the extensibility of the top and bottom actuator fabric layers. Four types of actuators were manufactured, each with different yarn type combinations for the top, middle, and bottom layers, as listed in Table 1, and according to the structure parameters listed in Table 2. A plain knitted structure, which was lightweight and less bulky, was selected as the base structure for all the actuators with the same dimensions (14 cm length and 2.5 cm width). To create contrasting material properties between the top layer and the other two layers (middle and top), the number of courses per centimeter (cpcm) of the former was selected to be higher than the latter

ones. This higher course-to-wale ratio between the top and bottom layers created a more extensible top layer due to the added extra rows of loops, which took the form of gathers at the top layer of all the actuators, as can be seen in Figure 1b. The use of yarn combinations of a highly extensible yarn such as Lycra with a less extensible yarn such as plied yarn for the top and bottom layers, respectively, was expected to create a range of anisotropy for the different actuators produced.

Table 1. Yarn combinations of actuator layers for each actuator type.

	Top Layer	Middle and Bottom Layer
Actuator Type 1	Lycra	Lycra
Actuator Type 2	Lycra	3-Ply Polyamide Yarn
Actuator Type 3	Lycra	Melting Yarn
Actuator Type 4	2-Ply Polyamide Yarn	3-Ply Polyamide Yarn

Table 2. Knitted structure parameters of the three actuator layers (common to all actuator types).

	Top Layer	Middle and Bottom Layer
Courses per cm (cpcm)	15	10
Wales per cm (wpcm)	5	5
Stitch density (S)	75	50
Course-to-wale ratio (ctwr)	15:5	10:5

To create an inflatable actuator, airtight tubes were fabricated using thermoplastic polyurethane stretchy film (Stretchlon 200, Fiber Glast). Each bladder was manufactured by laser cutting two identical (17 × 2.5 cm) rectangles, which were welded using an impulse sealer (PCS 300, Brother) from three edges. A polyurethane tube with a 6mm outer diameter was attached to the open edge of the bladder to connect it to the compressed air line. The tube was securely attached to the bladder with Globe PVC black tape in order to prevent any air leakage (Figure 1c). Finally, two identical bladders produced with the aforementioned technique were inserted in the top and bottom chambers in order to achieve flexion and extension motions, respectively, when inflated (Figure 1d).

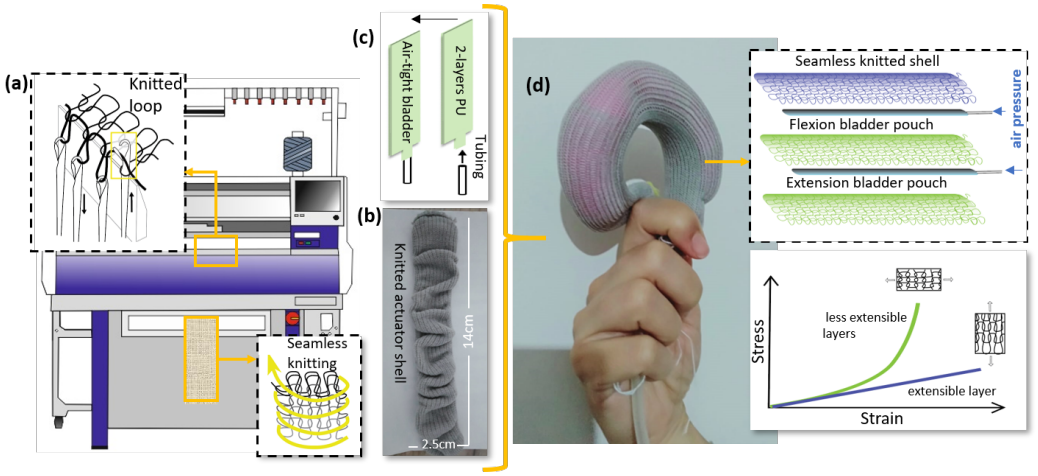

Figure 1. (**a**) Computerized flatbed whole-garment knitting. (**b**) Machine-knitted seamless actuator. (**c**) Polyurethane air-tight bladder assembly. (**d**) Bending motion of the knitted actuator under air pressurization and a construction principle based on an extensible top layer and less extensible middle and bottom layers.

3. Actuator Characterization

A portable control system, explained in Appendix A.1, was developed in order to characterize the bending motions of the developed knitted actuators. First, the actuator

was pressurized continuously up to 150 kPa using an air pump to achieve bending motion. The change in curvature values with respect to the applied pressure was recorded using a digital camera. To determine the actuator curvature in each video frame, an automated method based on edge detection and a circle fitting algorithm was used (Figure 2a). The detailed steps for calculating the curvature are discussed in Appendix A.2. This procedure was carried out six times for each actuator type, and as shown in Figure 2b, the knitted actuators exhibited consistent bending behavior when pressurized, and an approximately linear relationship between curvature and pressure was observed. It was clear that the different knitting parameters used to manufacture the actuators resulted in distinctively different bending behaviors. For example, Actuator Type 1 showed a maximum curvature of 21 m^{-1} (reciprocal of the SI unit for distance) at the maximum of 150 kPa of pressure applied due to the Lycra yarn used for knitting the whole actuator combined with the higher number of courses at the top layer. Although Actuator Types 3 and 4 showed the same curvature of 17.5 m^{-1} at a maximum pressure of 150 kPa, the initial curvature values for those actuators were different. It was also clear from the results that Actuator Type 4 exhibited the lowest curvature due to the absence of Lycra yarn in all layers of the actuator.

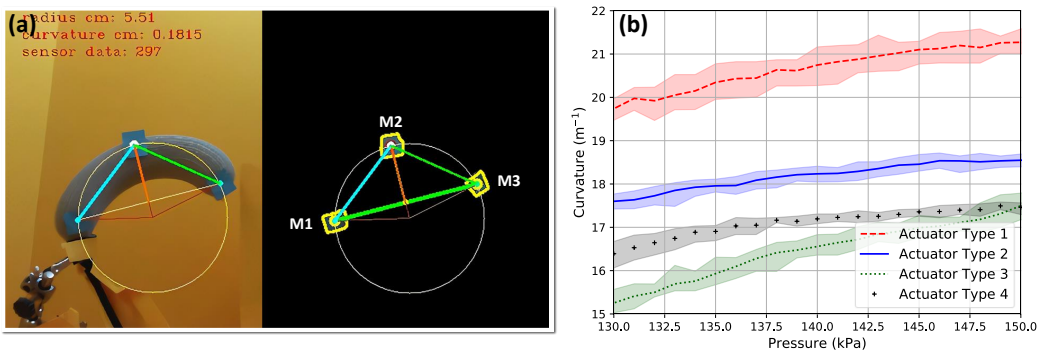

Figure 2. (**a**) Curvature measurement using a video frame. (**b**) Curvature of the seamless knitted actuators at different pressures.

Second, in order to deduce the force capacity of the knitted actuators, pressure values were correlated with the values of tip force, grip force, and output torque. To carry out the force measurements, experiment-oriented shapes were designed and fabricated using a 3D printer and placed on top of a digital dynamometer. While being pressurized, the free end of the actuator was applying pushing force on a cup-shaped object (Figure 3a) and a pulling force on a hollow rectangle (Figure 3c) attached to the dynamometer to measure tip and grip force, respectively. A torque test was carried out by placing the actuator in a hollow cylinder connected to the dynamometer (Figure 3e). The detailed steps for carrying out the tests are discussed in Appendix A.3. As the results in Figure 3b,d show, an approximately linear relationship was observed between tip and grip forces and the applied pressure for all four actuator types except for the dead-band region in Figure 3d, which occurred due to the actuator not applying any pulling force to the hollow rectangle attached to the dynamometer at the beginning of the pressurization. However, it was observed that the actuator types fell into different orders when the measured forces and curvature results at different pressures were compared. This indicated that the actuator with the higher curvature at a given pressure did not necessarily exert higher forces. For example, Actuator Type 1, which showed the highest curvature across the range of pressure applied, gave the lowest tip and grip forces compared to the other actuators. On the other hand, Actuator Type 3, which showed the lowest curvature, gave the highest tip force (5.3 N) and grip force (5 N), at the maximum pressure applied, compared to the other actuators. Actuator Type 3 was also tested for torque, given that it had the highest tip and grip force values. According to Figure 3f, our soft actuator was able to apply a torque that gradually increased up to bending values of about 45°, after which it started decreasing. One possible reason is the occurrence of the buckling phenomenon, which might negatively affect its performance.

In fact, it is known that buckling dramatically reduces the mechanical properties of a thin beam, leading to its failure for stresses much lower than those that might cause failure in a thicker beam. As the bending angle of the actuator increased, the compressive stresses in the side of the compressed fibers increased, causing a reduction in the maximum torque that it can apply. Nevertheless, this actuator exhibited a maximum torque value of 210 Nmm.

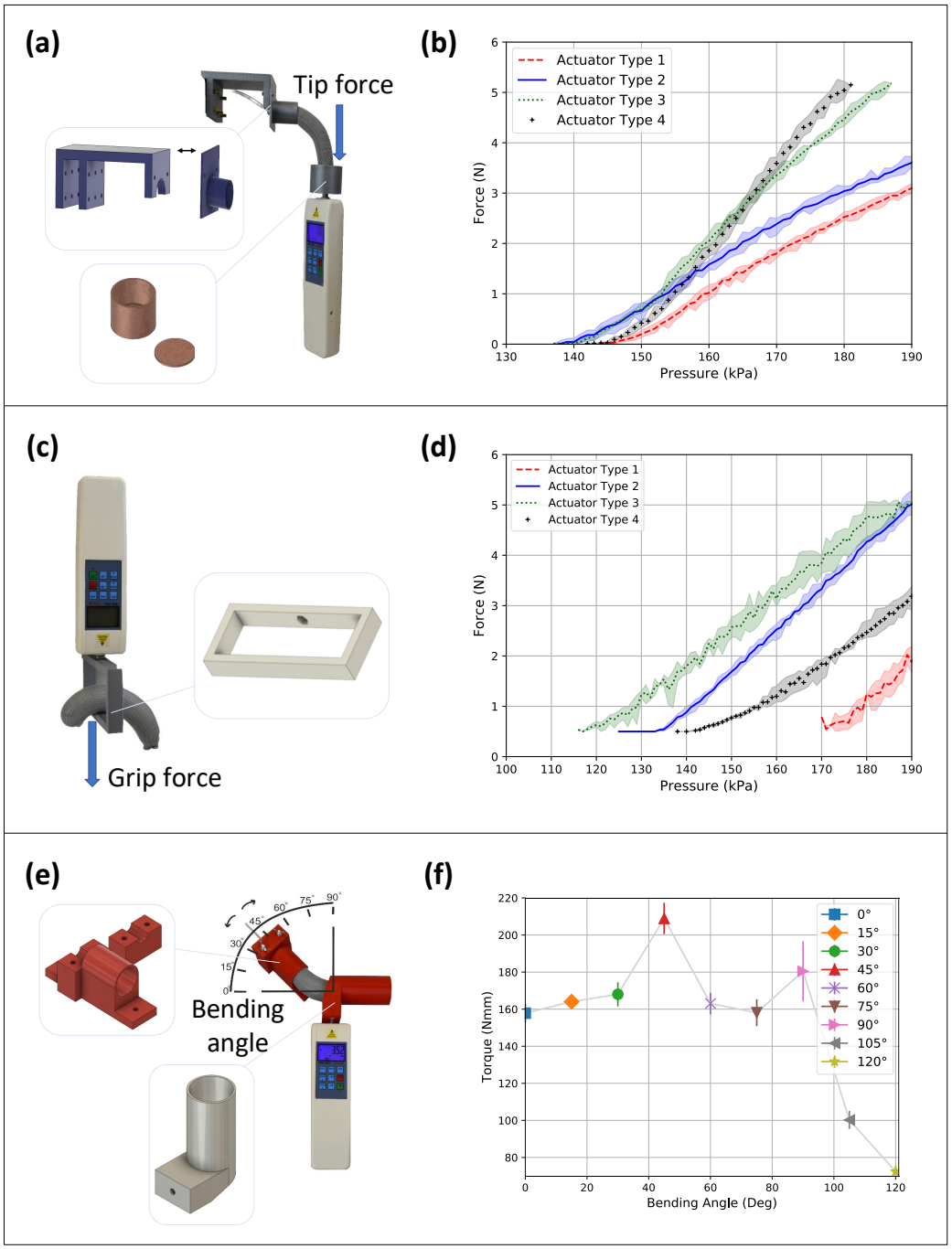

Figure 3. (**a**) Tip force test setup. (**b**) Tip force-pressure characteristics of all actuators. (**c**) Grip force test setup. (**d**) Grip force-pressure characteristics of all actuators. (**e**) Torque test setup. (**f**) Output torque of Actuator Type 3 at different bending angles.

The reported values above for the actuator curvature, grip and tip forces, and output torque were comparable to previously reported values measured for cut-and sew textile-based actuators at the 150 kPa applied pressure range [22–25]. However, in contrast to existing fabrication processes of textile-based actuators, the proposed seamless knitting

approach had a number of value-added features including; rapid, automated, and customizable manufacturing, less bulk and weight, robustness, and lower cost. Preliminary tests showed that a number of cut-and-sew actuators, manufactured based on currently used machine sewing techniques, did not withstand multiple pressure cycles due the bursting of seams (Appendix A.4). Furthermore, the single actuator can be incorporated into wearable structures for different body parts including hand, foot, or knee utilizing whole-garment knitting. Such an advancement would replace the use of multiple separate actuators as attachments on already-made garments into garment-like robotic structures. This would result in further reduction of bulk and weight. Endless machine knitting parameter combinations can be further explored in order to fine-tune the desired range and type of deformations. It must be highlighted that the parameter combinations chosen to produce the actuators in this study were arbitrarily selected to demonstrate the functionality of this manufacturing approach and provide a benchmark for a more in-depth investigation of seamless machine knitted actuators for various applications. Furthermore, higher gauge machines could be investigated as they would allow further reduction in the actuator form factor. A finer knitted fabric structure would also have a higher level of elasticity, which would ensure repeatable performance with multiple flexing and would be more compliant, therefore requiring lower pressure to achieve the desired deformation. All the aforementioned possible enhancements demonstrate the versatility of machine knitting and its potential for the development of wearable soft robotics structures.

4. Assistive Glove Demonstration

In order to demonstrate the potential of the seamless knitted actuators in wearable assistive device applications, they were integrated into an adjustable glove. Actuator Type 3, which exhibited the highest tip and grip forces, was selected. Five identical actuators were mounted on the top surface of the glove using Velcro belts and straps (Figure 4a). The test setup, detailed in Appendix A.1, for inflating and deflating the actuator was developed to control the five actuators via a computer according to preset air pressure values (see Supplementary Video S1). In order to evaluate the functionality of the glove, a range of flexion and extension actuator motions was set to allow grasping of different objects, as shown in Figure 4b. The results showed that the glove was capable of grasping objects, of different weights and sizes (up to 125 g), at the applied pressure range (up to 150 kPa).

Figure 4. (**a**) Wearable assistive glove prototype based on a seamless knitted actuator. (**b**) Achievable motions with the glove prototype for grasping objects of different weights and sizes.

In order to evaluate the assistive action of the glove, muscle activation was compared with and without the glove, while performing a sequence of hand actions. The sequence of actions included: (1) relaxing the hand, (2) closing the hand, (3) relaxing the hand again, and (4) opening the hand. To provide a reference point, these actions were then repeated without the glove while exerting maximal force in order to obtain the maximum voluntary contraction (MVC) percentage of the muscular activity, which can be defined as the maximum muscle strength. We avoided exerting any force in conducting the actions while

wearing the glove. Two EMG sensors (Advance Technologies MyoWare Muscle Sensor) with a sampling frequency of 50 Hz were placed on the flexor digitorum superficialis (FDS) and extensor digitorum communis (EDC) muscles (Figure 5a). The detected signal was later filtered with a second-order Butterworth filter with a critical frequency of 2 Hz. When worn, the glove was pressurized up to 150 kPa to complete the hand closing action and depressurized to relax the hand again in alternate sequence. As Figure 5b indicates, the maximum voluntary contraction (MVC) of both muscles while wearing the glove was at the baseline EMG activity. A significant muscle activity change was noted from 66.81% to 23.12% of MVC in the flexor muscle and from 35.49% to 21.33% of MVC in the extensor muscle, while closing and opening the hand. The results indicated that the user relied on the glove's auxiliary force to perform the actions.

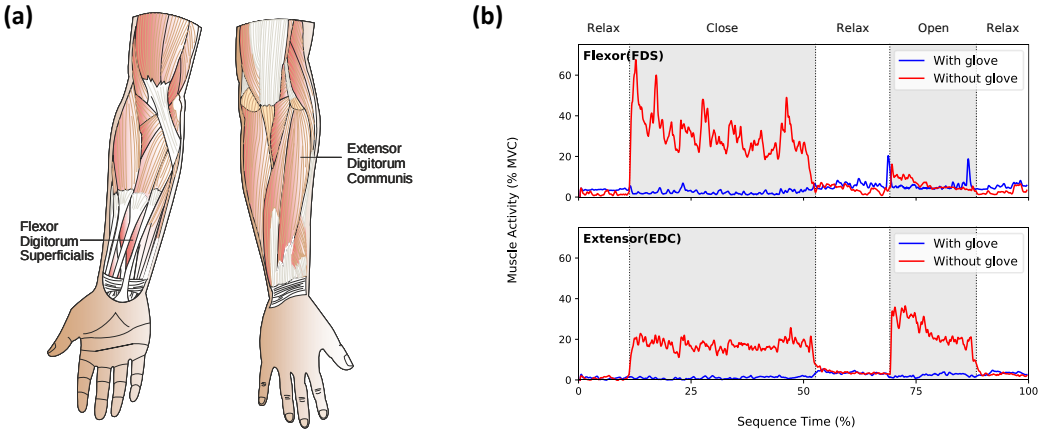

Figure 5. (**a**) EMG sensors' placement on arm muscles. (**b**) Muscle activity comparison with and without the powered glove.

5. Conclusions

In this work, we leveraged advanced computerized knitting to manufacture seamless pneumatic knitted actuators. An anisotropic fully knitted actuator structure was realized through combinations of machine knitting parameters. For the purposes of demonstrating the viability of the approach for manufacturing bending actuators, arbitrarily selected knitting parameters, including stitch density and yarn type variations for the top, middle, and bottom actuator layers, were investigated. The actuators were experimentally tested showing a range of bending curvatures, as well as grip and tip forces up to 5 N at a maximum 180 kPa air pressure value. The above-mentioned actuators were used to construct a wearable soft robotics glove, which aimed at assisting hand grasping motion. This application demonstrated the capability of the fully knitted actuators to exert sufficient force for grasping objects up to 125 g in weight at a minimal air pressure (150 kPa), comparable to existing cut-and-sew textile actuators. We believe that this cutting-edge approach, which to the best of our knowledge has not been presented before, will push the boundaries of garment-like wearable soft robotics manufacturing towards viable mass-production. Computerized whole-garment knitting, as demonstrated in this work, is an accessible technology for rapid iterations of textile actuators, which can be customized to different users. Further work will be carried out for investigating various combinations of knitting parameters in order to achieve higher ranges of actuator curvature and exerted forces at minimal pressure. The process will also be scaled up to manufacture a fully knitted glove and more complex garment geometries, which can be customized as assistive devices for different body parts. Another compelling potential advancement offered by this technology is the integration of textile-based sensors during the knitting process, which enables a two-way interaction between the user and the actuator through implementing closed-loop control strategies. All such advances would pave the way for complete systems of soft robotics garments.

Supplementary Materials: The following are available at https://www.mdpi.com/2076-0825/10/5/94/s1 , Video S1: Computer controlled assistive glove actuation. Video S2: Schematic of 10 inflation and deflation valves control. A supporting video article is available at doi: link.

Author Contributions: Conceptualization, A.T.A., G.I., O.A. and H.M.E.; methodology, A.T.A., L.C., H.M.E., A.F.Y., F.K. and K.O.; supervision, G.I. and O.A.; funding acquisition, G.I. and O.A.; project administration, G.I. and O.A.; writing—review and editing, G.I., O.A. and H.M.E.; writing—original draft, H.M.E., A.F.Y., F.K. and K.O.; data curation, K.O., F.K. and H.M.E.; formal analysis, K.O., F.K., A.F.Y. and H.M.E.; investigation, A.F.Y., K.O. and F.K.; resources, K.O., A.F.Y. and F.K.; software, F.K. and K.O.; visualization, F.K., K.O. and A.F.Y.; validation, A.T.A. and K.O. All authors read and agreed to the published version of the manuscript.

Funding: The authors disclose the receipt of the following financial support for research and authorship. This work was funded by EU Marie Skłodowska Curie IF Project "Textile based Soft Sensing Actuators for Soft Robotic Applications—TexRobots (Grant no: 842786)".

Institutional Review Board Statement: The study was approved by the Ethics Committee of Istanbul Technical University Human Medical and Engineering Research (SM-INAREK-2021-02).

Informed Consent Statement: Informed consent was obtained from all subjects involved in the study. Written informed consent was obtained from the patient to publish this paper.

Data Availability Statement: Data is contained within the article.

Acknowledgments: We are thankful for Hasan Hüseyin Gürbüz for his support in the test rig system, TETAŞ İÇ VE DIŞ TİC. A.Ş. for knit sample preparation, and Erhan Önal for the help with the EMG sensor. Hend M. Elmoughni, Ayse Feyza Yilmaz, Kadir Ozlem, and Fidan Khalilbayli contributed equally to this work.

Conflicts of Interest: The authors declare no conflict of interest. The funders had no role in the design of the study; in the collection, analyses, or interpretation of data; in the writing of the manuscript; nor in the decision to publish the results.

Abbreviations

The following abbreviations are used in this manuscript:

EDC	Extensor digitorum communis
EMG	Electromyography
FDS	Flexor digitorum superficialis
HSV	Hue saturation value
MVC	Maximum voluntary contraction
RGB	Red, green, blue
TTL	Transistor-Transistor Logic
USB	Universal Serial Bus

Appendix A.

Appendix A.1. Air Pressure Control System

A portable control system was developed in order to characterize the bending motions of the actuators. The system consisted of: (1) microcontroller, (2) relay card, (3) air pump, (4) valve driver cards, (5) solenoid valves, and (6) pressure sensors to inflate and deflate the actuators (Figure A1). Each valve controlled the inflation and deflation of each air bladder in order to achieve actuator bending and extension. The actuator motion was automatically controlled via a microcontroller using the on-off controller principle.

Real-time pressure values of each bladder were visualized through a graphical user interface via a computer. When the inflation button is pressed, air is pumped to inflate the bladder through the inflation valve. When the inflation valve is released, the current to the air pump and inflation valve is cut off, and the inflation of the actuator is stopped. The same procedure was conducted for the deflation operation. To achieve the bending motion of an actuator, the inflate valve of the flexion bladder and the deflate valve of the extension bladder are activated, which ensures that the flexion bladder is inflated while the extension bladder is deflated. When the bladders reach maximum inflation pressure,

the air pumping stops. The system was scaled up for glove actuation using a total of 10 inflation and 10 deflation valves (see Supplementary Video S2).

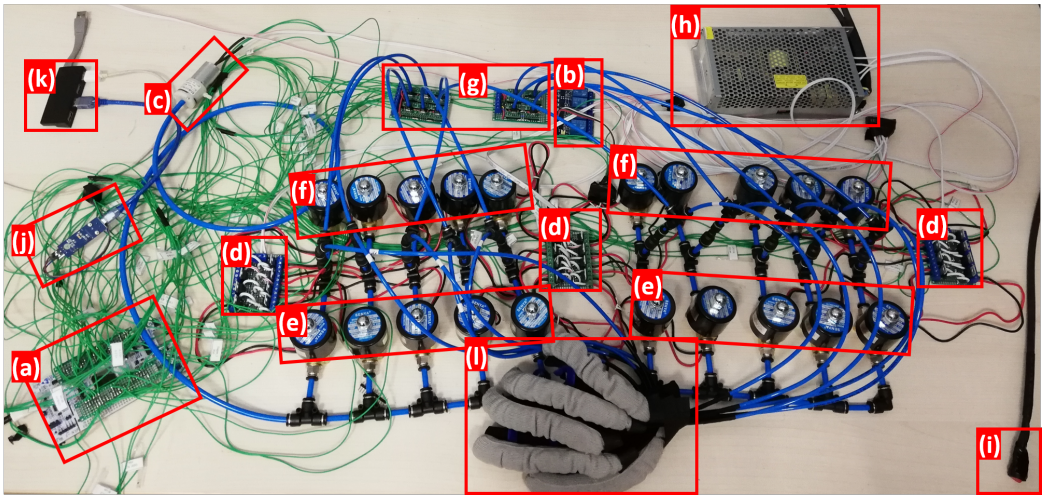

Figure A1. Air pressure control system components, which include: (**a**) Microcontroller. (**b**) Relay card. (**c**) Air pump. (**d**) Valve driver cards. (**e**) Inflate solenoid valves. (**f**) Deflate solenoid valves. (**g**) Pressure sensors. (**h**) Power supply. (**i**) Emergency stop switch. (**j**) USB to TTLconverter. (**k**) USB hub. (**l**) Soft robotic glove.

Appendix A.2. Curvature Test

The change in curvature values with respect to the applied pressure was recorded for each actuator type using a webcam (Microsoft LifeCam HD-3000, Microsoft, Beijing, China), which was positioned in alignment with the actuator plane. During the test, one end of the actuator was fastened to a stable stand, while the other end moved freely in a circular motion. Each actuator was continuously inflated up to 150 kPa and deflated six times consecutively. Since a color-based approach was implemented, the actuator was placed in a secluded area that was internally illuminated by LED strip lights, in order to avoid brightness variations along the actuator surface. To locate the actuator in each video frame, a marker-based solution was developed. Markers were placed on the extreme points along the actuator length, namely the bottom of the metacarpophalangeal (Marker 1), the top of the distal interphalangeal (Marker 2), and the middle of the proximal interphalangeal (Marker 3) joints (Figure 2a). In each captured frame, the RGB values were first converted into HSV to achieve better color-based image segmentation. To sooth the noise, dilation and erosion were applied to the resized and blurred frame. To detect the markers, outer contours and their respective center-of-mass covering the color range of the placed markers were located in the given frame. After identifying the intersection coordinate of Marker 3 and the line connecting Markers 1 and 2, the angle formed by Markers 3, 1, and the intersection pixels was determined. The radius of the possible circle created by the actuator movement (r) was calculated to be:

$$r = a \cdot cot(2x) + k \tag{A1}$$

where a is the distance between Marker 2 and intersection pixels, x is the aforementioned angle, and k is the distance between Marker 3 and intersection pixels. Curvature (c) was obtained from the equation $c = 1/r$. To represent the curvature value in terms of its actual length instead of pixels, an object with a known width and height was placed in the platform.

Appendix A.3. Tip and Grip Forces and Output Torque

A digital dynamometer (Geratech SH-50) was used in order to measure the forces and torque of the seamless knitted actuators. Data were transmitted to the computer via an RS-232 cable. Experiment oriented shapes were designed and fabricated using a 3D printer (Ultimaker 2+, Ultimaker, Zaltbommel, Netherlands) and placed on top of the dynamometer (Figure 4). Prior to starting the experiment, the actuators were fully pressurized and depressurized five times consecutively in order to eliminate any fabric or bladder relaxation and to fit the actuators to the custom test rig. One end of the actuator was fastened to a custom-made board, while the other end moved freely in a circular bending motion, to avoid any undesired movements, which would result in noise. While being pressurized, the free end of the actuator was applying a pushing force on the cup-shaped object and a pulling force on the hollow rectangle attached to the dynamometer to measure tip and grip forces, respectively. For torque measurement, the actuator was placed in a hollow cylinder connected to the dynamometer. The actuator was pressurized up to 150 kPa and placed from the other end at angles between 0° and 120° subsequently, in multiples of 15 (Figure A2). Output torque was calculated as the product of the pressure value obtained from the dynamometer and the distance between the actuator and the dynamometer at each angle.

Figure A2. Output torque measurement setup.

Appendix A.4. Bursting of Cut-and-Sew Actuators

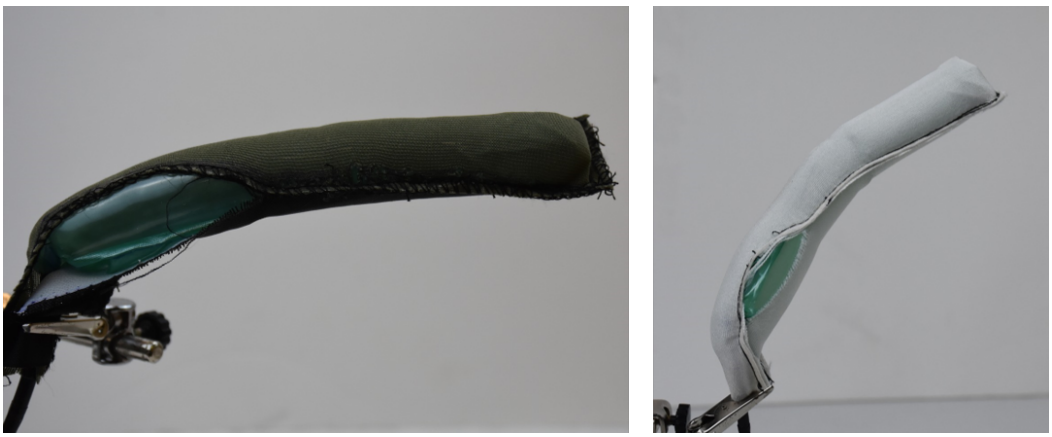

Figure A3. Cut-and-sew actuators bursting upon pressurization.

References

1. Thalman, C.; Artemiadis, P. A review of soft wearable robots that provide active assistance: Trends, common actuation methods, fabrication, and applications. *Wearable Technol.* **2020**, *1*, E3. [CrossRef]
2. Cianchetti, M.; Laschi, C.; Menciassi, A.; Dario, P. Biomedical applications of soft robotics. *Nat. Rev. Mater.* **2018**, *3*, 143–153. [CrossRef]
3. Polygerinos, P.; Correll, N.; Morin, S.A.; Mosadegh, B.; Onal, C.D.; Petersen, K.; Cianchetti, M.; Tolley, M.T.; Shepherd, R.F. Soft robotics: Review of fluid-driven intrinsically soft devices; manufacturing, sensing, control, and applications in human-robot interaction. *Adv. Eng. Mater.* **2017**, *19*, 1700016. [CrossRef]
4. Yap, H.K.; Lim, J.H.; Nasrallah, F.; Yeow, C.H. Design and preliminary feasibility study of a soft robotic glove for hand function assistance in stroke survivors. *Front. Neurosci.* **2017**, *11*, 547. [CrossRef] [PubMed]
5. Jung, J.C.; Jang, J.H.; Rodrigue, H. Inflatable L-shaped prisms as soft actuators for soft exogloves. *Eng. Res. Express* **2019**, *1*, 025009. [CrossRef]
6. Yang, Y.; Wu, Y.; Li, C.; Yang, X.; Chen, W. Flexible actuators for soft robotics. *Adv. Intell. Syst.* **2020**, *2*, 1900077. [CrossRef]
7. Zhong, G.; Hou, Y.; Dou, W. A soft pneumatic dexterous gripper with convertible grasping modes. *Int. J. Mech. Sci.* **2019**, *153*, 445–456. [CrossRef]
8. Sun, Y.; Zhang, Q.; Chen, X. Design and analysis of a flexible robotic hand with soft fingers and a changeable palm. *Adv. Robot.* **2020**, *34*, 1041–1054. [CrossRef]
9. Sanchez, V.; Walsh, C.J.; Wood, R.J. Textile Technology for Soft Robotic and Autonomous Garments. *Adv. Funct. Mater.* **2021**, *31*, 2008278. [CrossRef]
10. Persson, N.K.; Martinez, J.G.; Zhong, Y.; Maziz, A.; Jager, E.W. Actuating textiles: Next generation of smart textiles. *Adv. Mater. Technol.* **2018**, *3*, 1700397. [CrossRef]
11. Belforte, G.; Eula, G.; Ivanov, A.; Sirolli, S. Soft pneumatic actuators for rehabilitation. *Actuators* **2014**, *3*, 84–106. [CrossRef]
12. Cappello, L.; Meyer, J.T.; Galloway, K.C.; Peisner, J.D.; Granberry, R.; Wagner, D.A.; Engelhardt, S.; Paganoni, S.; Walsh, C.J. Assisting hand function after spinal cord injury with a fabric-based soft robotic glove. *J. Neuroeng. Rehabil.* **2018**, *15*, 1–10. [CrossRef] [PubMed]
13. Yap, H.K.; Khin, P.M.; Koh, T.H.; Sun, Y.; Liang, X.; Lim, J.H.; Yeow, C.H. A fully fabric-based bidirectional soft robotic glove for assistance and rehabilitation of hand impaired patients. *IEEE Robot. Autom. Lett.* **2017**, *2*, 1383–1390. [CrossRef]
14. Low, J.; Cheng, N.; Khin, P.; Thakor, N.V.; Kukreja, S.L.; Ren, H.; Yeow, C.H. A bidirectional soft pneumatic fabric-based actuator for grasping applications. In Proceedings of the 2017 IEEE/RSJ International Conference on Intelligent Robots and Systems (IROS), Vancouver, BC, Canada, 24–28 September 2017; pp. 1180–1186.
15. Al-Fahaam, H.; Davis, S.; Nefti-Meziani, S.; Theodoridis, T. Novel soft bending actuator-based power augmentation hand exoskeleton controlled by human intention. *Intell. Serv. Robot.* **2018**, *11*, 247–268. [CrossRef]
16. Connolly, F.; Wagner, D.A.; Walsh, C.J.; Bertoldi, K. Sew-free anisotropic textile composites for rapid design and manufacturing of soft wearable robots. *Extrem. Mech. Lett.* **2019**, *27*, 52–58. [CrossRef]
17. Visan, A.L.; Alexandrescu, N.; Belforte, G.; Eula, G.; Ivanov, A. Experimental researches on textile laminate materials. *Ind. Textila* **2012**, *63*, 315–321.
18. Cappello, L.; Galloway, K.C.; Sanan, S.; Wagner, D.A.; Granberry, R.; Engelhardt, S.; Haufe, F.L.; Peisner, J.D.; Walsh, C.J. Exploiting textile mechanical anisotropy for fabric-based pneumatic actuators. *Soft Robot.* **2018**, *5*, 662–674. [CrossRef] [PubMed]
19. Ray, S.C. *Fundamentals and Advances in Knitting Technology*; CRC Press: Boca Raton, FL, USA, 2012.
20. Spencer, D.J. *Knitting Technology: A Comprehensive Handbook and Practical Guide*; Woodhead Publishing: Sawston, Cambridge, UK, 2001.
21. McCann, J.; Albaugh, L.; Narayanan, V.; Grow, A.; Matusik, W.; Mankoff, J.; Hodgins, J. A compiler for 3D machine knitting. *ACM Trans. Graph. (TOG)* **2016**, *35*, 1–11. [CrossRef]
22. Correia, C.; Nuckols, K.; Wagner, D.; Zhou, Y.M.; Clarke, M.; Orzel, D.; Solinsky, R.; Paganoni, S.; Walsh, C.J. Improving Grasp Function After Spinal Cord Injury With a Soft Robotic Glove. *IEEE Trans. Neural Syst. Rehabil. Eng.* **2020**, *28*, 1407–1415. [CrossRef] [PubMed]
23. Zhou, Y.M.; Wagner, D.; Nuckols, K.; Heimgartner, R.; Correia, C.; Clarke, M.; Orzel, D.; O'Neill, C.; Solinsky, R.; Paganoni, S.; others. Soft robotic glove with integrated sensing for intuitive grasping assistance post spinal cord injury. In Proceedings of the 2019 International Conference on Robotics and Automation (ICRA), Montreal, QC, Canada, 20–24 May 2019; pp. 9059–9065.
24. Yap, H.K.; Ang, B.W.; Lim, J.H.; Goh, J.C.; Yeow, C.H. A fabric-regulated soft robotic glove with user intent detection using EMG and RFID for hand assistive application. In Proceedings of the 2016 IEEE International Conference on Robotics and Automation (ICRA), Stockholm, Sweden, 16–21 May 2016; pp. 3537–3542.
25. Ge, L.; Chen, F.; Wang, D.; Zhang, Y.; Han, D.; Wang, T.; Gu, G. Design, modeling, and evaluation of fabric-based pneumatic actuators for soft wearable assistive gloves. *Soft Robot.* **2020**, *7*, 583–596. [CrossRef] [PubMed]